2018年1月30日
六本木 泉ガーデンタワー（東京）

第35回無機材料に関する最近の研究成果発表会

ガラス研磨モデルの界面計測に基づく化学機械研磨メカニズムの提案

静岡大学大学院
総合科学技術研究科
須田 聖一
suda@shizuoka.ac.jp

1

Introduction
– Application of ultra-smooth glasses –

Ultra-smooth glasses

HOYA HP　　AGC HP

Hard disk glass substrates　Flat panel displays　*etc.*

Fig. 1. Application of ultra-smooth glasses.

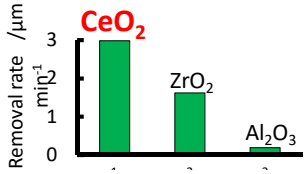

Lee M. Cook, J. Non-Crystalline Solids, **120**, 152-171(1990).

Fig. 2. Removal rate of glasses using conventional abrasives.

CeO_2 abrasives

Scratch-free glass surface and high removal rate

(Mechanism)

⇨ **Chemical Mechanical Polishing (CMP)**

2

Introduction
– High polishing properties of ceria abrasives –

Chemical Mechanical Polishing (CMP)

Excellent polishing properties of the **ceria-based abrasives** are brought by chemical mechanical polishing (CMP).

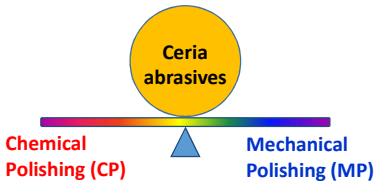

Fig. 3. Image view of cooperation between chemical polishing and mechanical polishing.

Zirconia or alumina shows superior mechanical strength, but glass polishing properties are much inferior to ceria abrasives.

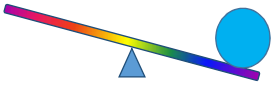

Fig. 4. Image view of polishing CP/MP balance on zirconia or alumina abrasives.

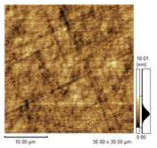

Glasses polished with alumina or zirconia often observe relatively deep scratches.

Fig. 5. AFM image of glass after polishing with conventional zirconia particles.

3

Introduction
– Previously Proposed CP Mechanism –

Covalent Bonding Formation CP Mechanism proposed by Dr. Hoshino *et.al.*

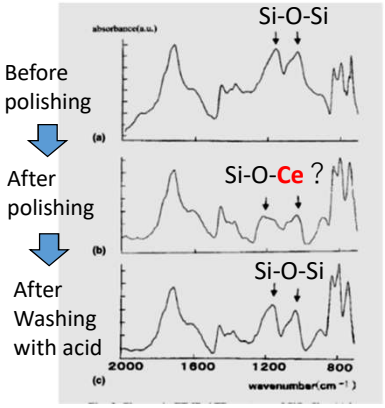

T. Hoshino, Y. Kurata, Y. Terasaki, K. Susa, J. Non-Cryst. Solids, **283**, 129-136 (2001).

Fig. 6. FT-IR spectra of glasses before and after polishing with ceria abrasives.

$Ce\text{-}OH + Si\text{-}O^- \leftrightarrow Si\text{-}O\text{-}Ce + OH^-$

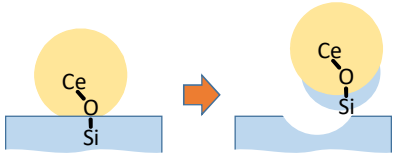

Fig. 7. Image view of removing Si-O on the surface of glass by ceria abrasives.

SiO_2 surface is first reacted with CeO_2 particles and a multiple number of chemical bondings of Si-O-Ce are formed on the surface.
SiO_2 is removed as a lump, which is scraped from the surface. The polishing rate is affected by **the formation of Ce-O-Si bonding**.

4

Introduction
– Proposing CP mechanism with ceria abrasives –

Charge Transfer Chemical Polishing (CP) Mechanism

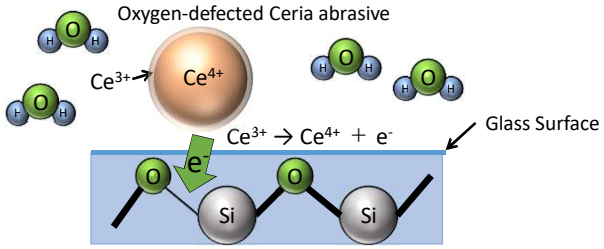

Fig. 8. Image view of hydration formation of glass surface according to charge transfer CP mechanism.

1. Electrons formed by oxidation of Ce^{3+} will transfer to anti-bonding orbital of Si-O during polishing.
2. The charged electrons in the orbitals extend Si-O bond distance and weaken the bonds.

5

Introduction
– Overview of glass CMP process –

Chemical Process of CMP

Producing hydration layers on glass.

Mechanical Process of CMP

Sweeping softened hydration layers off glass.

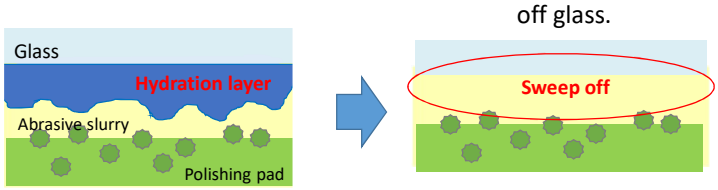

Fig. 9. Schematic illustration of proposed glass CMP processes.

Polishing properties such as removal rate and surface smoothness would much depend on formation rate of hydration layer on glass.

Quantitative estimation of hydration layer during CMP is important to clarify CMP mechanism and to develop novel CMP abrasives.

6

Introduction
– Proposed hydration layer formation mechanism–

Surface of ceria abrasives $Ce^{3+} \rightarrow Ce^{4+} + e^-$

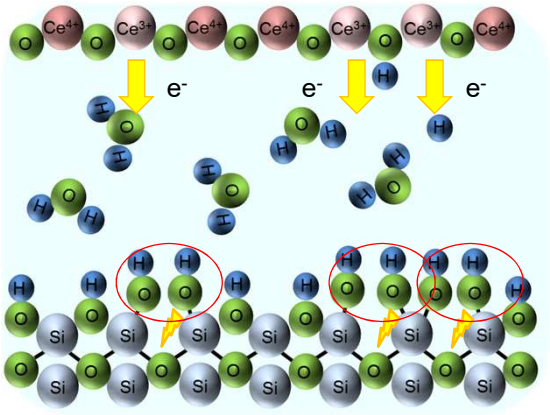

Glass surface

Challenge 1: Abrasive surface conditions by estimating abrasive/water interfacial resistance.

Challenge 2: Effects of ions in water solution on hydration and removal rate.

Challenge 3: Hydration layers by estimating water/glass interfacial resistance.

Challenge 4: Hydration layers by estimating electric potential between ceria and water.

7

Challenge 1: Abrasive surface conditions by estimating abrasive/water interfacial resistance.

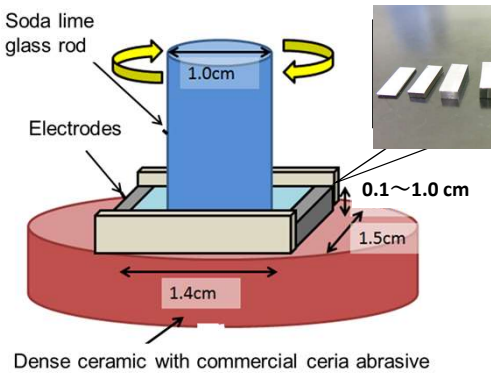

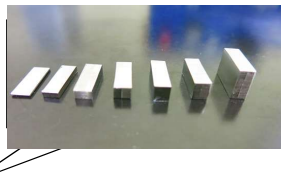

Electrodes： SUS304
Height, ***h***： 0.1～1.0 cm

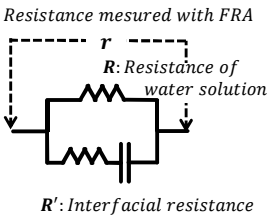

Fig. 10. Schematic illustration for estimation of electrical properties of abrasive/water interfacial resistance during polishing.

8

Challenge 1: Experiments
– Estimation of interfacial resistance during polishing –

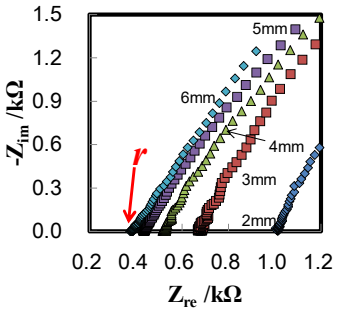

Fig. 11. Typical complex impedance profiles using various electrodes.

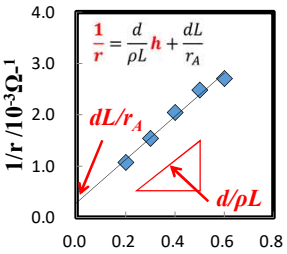

Fig. 12. Relationship between the reciprocal of resistance and height of electrodes.

Resistance mesured with FRA

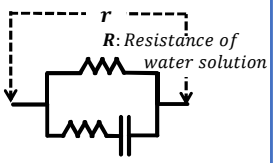

R': *Interfacial resistance*

$$\frac{1}{r}=\frac{1}{R}+\frac{1}{R'}$$

$$\Rightarrow \frac{1}{r}=\frac{d}{\rho L}h+\frac{dL}{r_A}$$

ρ: *Resistivity of water solution*

r_A: *Interfacial area specific resistance (ASR)*

Linear relationship enables us to estimate ρ (Resistivity of water solution) and r_A (ASR) separately.

Challenge 1: Results
– Change in solution resistivity and abrasives/water ASR –

Resistivity of water solution

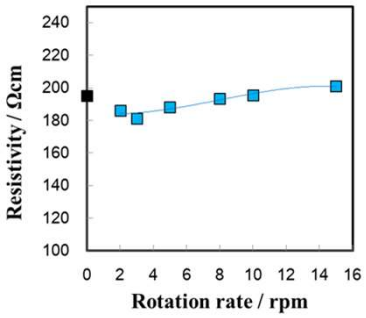

Fig. 13. Relationship between solution resistivity and rotation rate.

Interfacial ASR

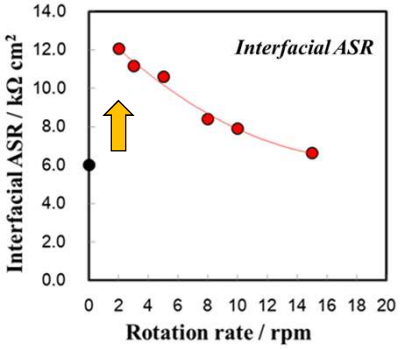

Fig. 14. Relationship between abrasive/water interfacial ASR and rotation rate.

The ASR was doubled by starting rotation of soda-lime glasses. Ceria surface would be changed by polishing in association with migration of charge carrier.

Challenge 2: Results
– Effects of NH_4NO_3 concentration –

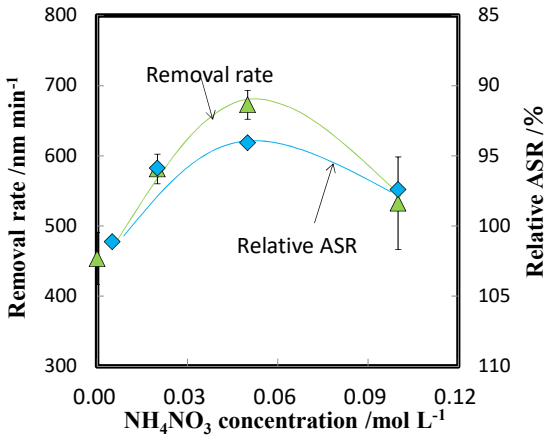

< 0.05 mol L^{-1}

Hydration layer ↑

Removal rate ↑

> 0.05 mol L^{-1}

Hydration layer ↓

Removal rate ↓

Fig. 15. Relationship between removal rate or relative ASR and NH_4NO_3 concentration in the slurry.

11

Challenge 2: Discussion
– Effects of NH_4NO_3 concentration –

NH_4NO_3 concentration

<0.05 mol L^{-1} | **>0.05 mol L^{-1}**

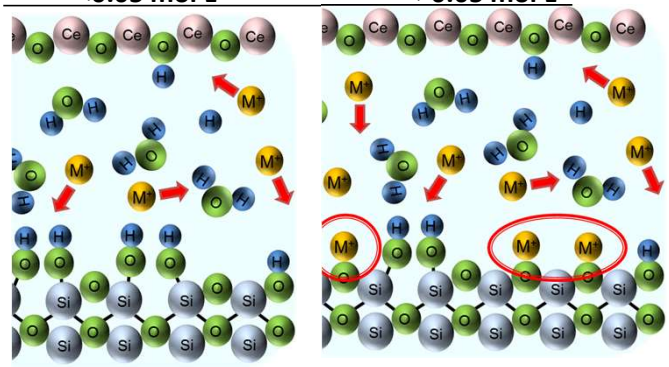

Small amount addition of NH_4NO_3 would increase electron charge carrier density in slurry and improves removal rate However, excess addition of charge carrier ions would inhibit hydration reaction by steric hindrance.

Fig. 16. Schematic illustration model of promoted hydration reaction with water solution at less than 0.05 mol L^{-1} NH_4NO_3.

Fig. 17. Schematic illustration model of inhibited hydration reaction with water solution at more than 0.05 mol L^{-1} NH_4NO_3.

12

Challenge 3: Experiments
– Setup for water/glass interfacial ASR measurement –

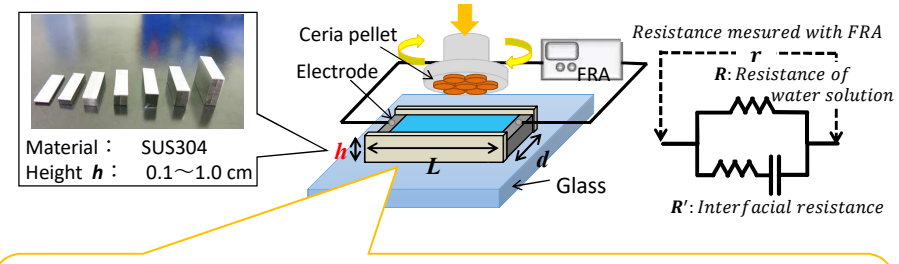

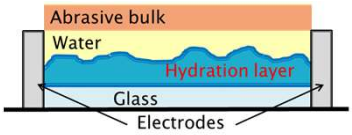

Abrasive：0, 20, 40% La doped CeO_2 (**LDC00, 20, 40**), ZrO_2 (**ZR**), Commercial ceria abrasive (**ComCe**)

Water solution: 0.02 ～ 0.10 mol $L^{-1}NH_4NO_3$ solution

Fig. 18. Schematic illustration for estimation of electrical properties of glass/water interfacial hydration layer during polishing.

13

Challenge 3: Results
– Temperature dependence of conductivity and ASR –

Conductivity of water solution

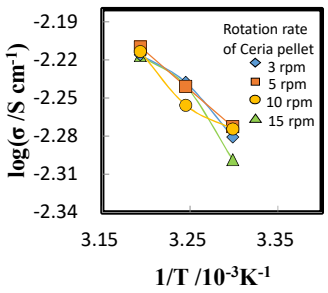

Fig. 19. Temperature dependence of water solution conductivity during polishing.

Interfacial ASR

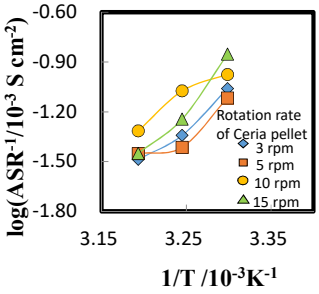

Fig. 20. Temperature dependence of Interfacial conduction (1/ASR).

Temp. → Water solution *vs.* Interface

14

Challenge 3: Results
– Impact of rotation –

Resistivity of water solution

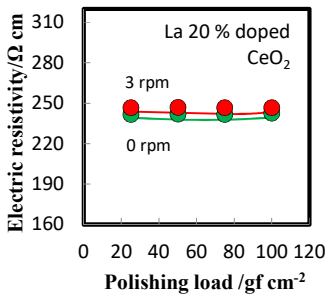

Fig. 21. Relationship between water solution resistivity and load during polishing.

Interfacial ASR

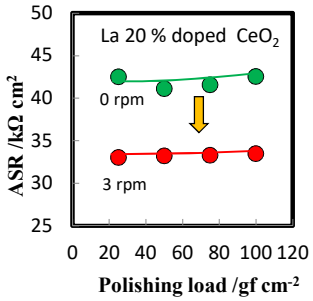

Fig. 22. Relationship between interfacial ASR and load during polishing.

Hydration layer would be promoted by polishing (both load and rotation of ceria pellet).

15

Challenge 3: Discussion
– Removal rate vs. Polishing load –

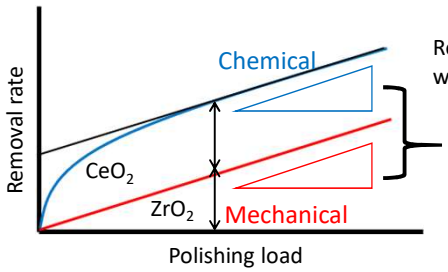

T. SAWANO, T. MARUYAMA, Y. MORIWAKI, Proc. 2013 JSPE Spring Meeting, 655 (2013).

Fig. 23. Illustration of effect of polishing load on removal rate for CeO_2 and ZrO_2 abrasives.

Removal rate increases with increasing polishing load

Both slopes coincide.

Chemical process of CMP (chemical polishing) is independent of load during polishing.

Hydration layer is formed with shear stress during polishing, but amount of hydration would be independent of polishing loads.

16

Challenge 3: Results
– Impact of ceria abrasive composition –

Solution resistivity

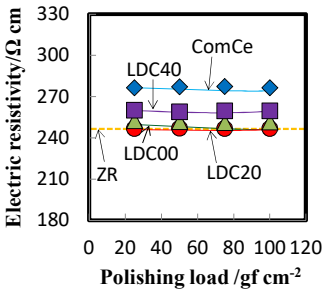

Fig. 24. Relationship between polishing loads and solution resistivity for various abrasives.

Interfacial ASR

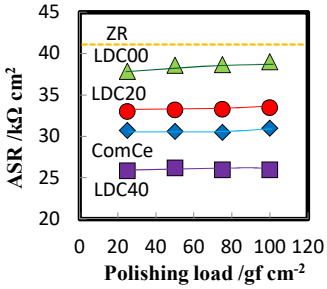

Fig. 25. Relationship between polishing loads and interfacial ASR for various abrasives.

La doping → *slightly* Solution resistivity *vs.* Interfacial ASR

17

Challenge 3: Results
– La contents vs. removal rate and hydration layer –

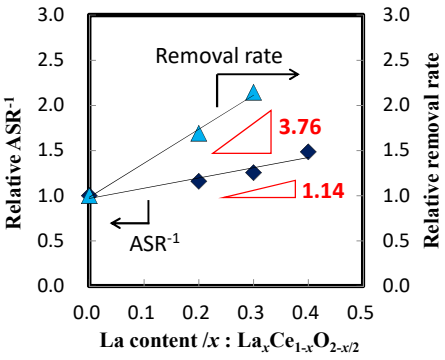

Fig. 26. Relationship between La concentration in CeO_2 and removal rate or ASR.

La doping → Hydration layer *vs.* Removal rate

Linear relationship between the La contents and relative ASR^{-1} .

The slope of hydration formation is approximately 1 and that of removal rate is 3.8.

Formation of hydration layer would be effective to improve polishing properties.

18

Challenge 4: Experiments
– Setup for electric potential measurement –

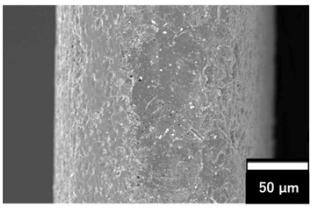

Fig. 27. SEM image of dense CeO_2 ceramic plate used for the estimation of electric potential.

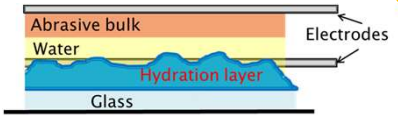

Abrasive：pure CeO_2 (**LDC00**)
Water solution: 0.05 mol $L^{-1}NH_4NO_3$ solution

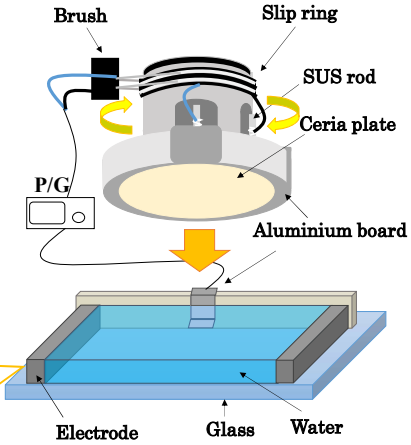

Fig. 28. Schematic illustration for estimation of electric potential voltage during polishing.

19

Challenge 4: Results
– Electric potential measurement –

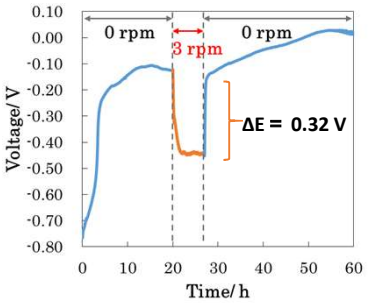

Fig. 29. Change in potential voltage with time.

Revision of evaluation system led to be reproducible data on potential change.

$\Delta E = 0.32$ V → $\Delta G = -31.1$ kJ/mol

Hydration free energy of soda lime glass
C. M. Jantzen, M. J. Plodinec, J. Non-Cryst. Solids, **67**, 207-223 (1984).
→ -27～－41 kJ/mol

The measured ΔG is closed to the hydration free energy of soda lime glass.

These ASR and electric potential would directly exhibit hydration reaction.

20

Discussion

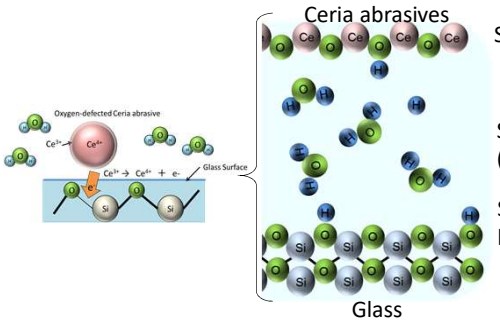

Step 1. Charge transfer with Ce^{3+}/Ce^{4+}.

Step 2. Diffusion of ions (electron carrier).

Step 3. Charge transfer and hydration on the surface of glass.

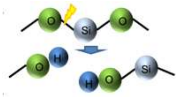

Fig. 30. Schematic illustration of proposed elementary chemical reactions during chemical polishing.

Step 1 would be rate-limiting of chemical polishing. Abrasive composition and inducing share stress much depend on hydration layer formation on the surface of glasses.

21

Summary

Quantitative elucidation of CMP is indispensable to improve polishing rate and develop novel abrasives. We investigated the estimation of hydration layer during polishing by measuring interfacial ASR and electric potential during polishing.

1. Hydration layer is formed with shear stress during polishing, but amount of hydration would be independent of polishing loads.

2. Amount of hydration layer could be estimated using reciprocal of ASR. The good linear relationship was observed between lanthanum contents and relative value of reciprocal of ASR and removal rate.

3. The hydration reaction was detected by measuring change in electric potential by inducing share stress.

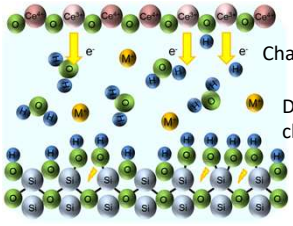

Fig. 31. Schematic illustration of three elementary reactions by chemical polishing.

22